RESEARCH MEMORANDUM

(2)

EXPERIMENTAL INVESTIGATION OF FLOW THROUGH THREE HIGHLY LOADED INLET GUIDE VANES HAVING DIFFERENT SPANWISE CIRCULATION GRADIENTS

By Loren A. Beatty, Melvyn Savage, and James C. Emery

Langley Aeronautical Laboratory
Langley Field, Va.

NATIONAL ADVISORY COMMITTEE FOR AERONAUTICS

WASHINGTON

July 28, 1952

1M NACA RM L52D25a

NATIONAL ADVISORY COMMITTEE FOR AERONAUTICS

RESEARCH MEMORANDUM

EXPERIMENTAL INVESTIGATION OF FLOW THROUGH THREE HIGHLY LOADED INLET GUIDE VANES HAVING DIFFERENT SPANWISE CIRCULATION GRADIENTS

By Loren A. Beatty, Melvyn Savage, and James C. Emery

SUMMARY

Three highly loaded inlet guide vanes for an axial-flow compressor were designed and tested in a low-speed annular cascade. The guide vanes included a free-vortex design, a solid-body design, and one with a design tangential velocity distribution which showed a greater increase with radius than the solid-body type. The last two guide vanes had very large amounts of radial flow. A comparison between design and measured turning angles was made by neglecting the induced effects of secondary flow phenomena and later by taking them into account by the method of Lieblein and Ackley, NACA RM E51G27.

The measured turning angles for all three guide vanes in the regions where secondary flow effects were negligible were always greater than the two-dimensional cascade turning angles (in some instances as much as 3°) reported by Zimney and Lappi, NACA ACR L5G18. Measured turning angles as much as 7° below the design angles can result over the outboard 30 percent of the vane if the induced effects of secondary flows are ignored in designing highly loaded inlet guide vanes with large radial circulation gradients (hub axial velocity approximately three times greater than those at the tip section). The Lieblein and Ackley method for correcting design turning angles for the effects of secondary flow gave good agreement between measured and corrected design turning angles for guide vanes having large variations in axial velocity.

The total pressure loss associated with guide vanes having a large amount of radial flow (hub axial velocity two or three times greater than that at the tip) is somewhat greater than that for a free-vortex guide vane. The use of guide vanes as highly loaded as these is not recommended in a compressor design until the effects of such highly loaded guide vanes on the succeeding rotor performance are known.

INTRODUCTION

The present trend in axial-flow-compressor design is toward higher-pressure-ratio, higher-mass-flow designs which require higher rotational speeds and higher blade Mach numbers. The rotor-tip inlet Mach number generally limits compressor rotational speed and, therefore, stage pressure ratio. In order to permit high rotational speeds to be used, guide vanes having tangential velocity distributions which increase with radius are used to prerotate the flow entering the first set of rotor blades. Guide vanes with this type of tangential velocity distribution have radial circulation gradients and radial flows which produce induced velocities that alter the measured turning angles. These effects were generally ignored in most guide-vane design work. The resulting discrepancies between design and measured turning angles may cause severe mismatching of blade rows which can adversely affect the over-all compressor efficiency and the accurate prediction of the compressor design point. A correction system for determining the effect of secondary flows on design turning angles of inlet guide vanes is presented in reference 1. This system ultilizes a suitable distribution of trailing vortices and vortex sheets in order to yield an induced turning angle representing the effects of the guide-vane radial circulation gradient and end-wall boundary layers. Reference 1 indicates that the correction system used in conjunction with two-dimensional cascade data gave very good agreement between corrected design and measured turning angles for several guide vanes having different radial circulation gradients with the maximum design radial variation of axial velocity being no greater than 17 percent.

In order to obtain the high rotational speeds and mass flows that are desirable within the Mach number limitation of present rotor blade sections, the use of highly loaded guide vanes which may have design radial variations in axial velocity much greater than 17 percent is necessary. Because of the interest in guide vanes of this kind, unreported data for three highly loaded guide vanes tested several years ago have been assembled for analysis. Design tangential velocity distributions include a free-vortex type, a solid-body type, and one which has a greater radial gradient of tangential velocity than the solid-body type. The last two guide vanes had large radial gradients in circulation and large amounts of radial flow, and

they represent loadings which are at or possibly beyond the upper limit of practical use. Recent unpublished data indicate that there is a guide-vane loading limit above which stage efficiency can be adversely affected. These very highly loaded guide vanes were designed to show the applicability of simple equilibrium, two-dimensional cascade data, and secondary flow-effect correction for guide-vane design at the extreme end of high loading. The use of guide vanes as highly loaded as these is not recommended in a compressor design until the effects of such highly loaded guide vanes on the succeeding rotor performance are known.

Measurements of total pressure, static pressure, and flow direction were made downstream of the guide vane; also a comparison between design and measured turning angles and exit velocities was made. The design turning angles were corrected for three-dimensional induced effects by the method of reference 1 and the results were compared with the measured turning angles to determine the effectiveness of the correction method in guide vanes having large variations in axial velocity. Sufficient data were taken so that contour plots of total pressure loss across the guide vane could be drawn.

APPARATUS AND PROCEDURE

Annular Cascade

The apparatus used to obtain the test data presented was a nontapered annular cascade with a 20-inch outer casing diameter and 10-inch inner casing diameter. (See fig. 1.) For all tests, 24 blades were used. Solidities varied from 1.44 to 1.50 from hub to tip, respectively, for the free-vortex guide vane and a constant solidity of 1.50 was used for the other guide vanes. The tests were made at a Reynolds number of approximately 100,000, corresponding to inlet axial velocities of about 65 feet per second. Ambient air was taken from the room by a large low-speed centrifugal blower and forced into a settling chamber from which it passed through three 40-mesh wire screens into a contracting section which faired into the bell-mouth inlet of the cascade. The hub was supported by 4 streamlined struts which were attached to the outer casing of the bell-mouth inlet. The guide vanes being tested were bolted at the tip end to a wooden ring which was mounted just downstream of the bell-mouth inlet. Because of the method of assembly of the cascade, the

hub end of the vanes was not fastened to the hub of the cascade; hence, it was necessary to provide a smooth junction and a tight seal in order to eliminate leakage losses and any unnecessary surface losses. The constant-area passage was maintained downstream of the vanes for approximately 17 inches before returning the air to the room.

Instrumentation

Survey stations were located approximately 2 inches upstream and downstream of the vanes. Surveys downstream of the vanes for total pressure, static pressure, and flow direction were made at approximately 30 radial stations at each of 13 circumferential positions equally spaced across two passages for each vane tested. Upstream of the vanes, survey measurements were made at approximately 20 radial stations at one circumferential position. Survey stations downstream were carefully located so as not to be influenced by the wakes from the upstream support struts. At the downstream survey stations the assumption was made that radial velocities were negligible, that is, simple equilibrium had already been established. (See ref. 2.) The survey instrument was constructed so that, at all measuring stations, it extended radially across the annular passage into a circumferential slot in the inner casing. All survey measurements were made with a cylindrical-type probe of $\frac{1}{4}$-inch diameter with 3 taps spaced 30° apart. (See fig. 2.) Yaw measurements were made by use of the two taps 60° apart while total head was obtained from the third tap; static pressure was obtained by a calibration of the reading from the yaw taps. This method was found to be sufficiently accurate for the low speeds at which these tests were made. Measuring accuracy was determined to be ±0.5° for turning angles and ±3.0 percent for velocities.

Blade Design

The three highly loaded entrance guide vanes were originally designed with design I having a free-vortex type of tangential velocity distribution from hub to tip $\left(V_u \propto \frac{1}{r}\right)$ and designs II and III having solid-body distributions ($V_u \propto r$). With a knowledge of the tangential velocity distribution, the axial velocity distribution leaving the guide vane may be calculated by use of the following equation derived in reference 3:

$$V_{a_2}^2 = V_{a_{2_m}}^2 + V_{u_{2_m}}^2 - V_{u_2}^2 - 2\int_{r_m}^{r} \frac{V_{u2}}{r}\,dr$$

where V_{a_2} is the guide-vane exit axial velocity at any radius, V_{u_2} is the guide-vane tangential velocity at any radius, and r is the radial position. (Subscript m indicates mean radius location.) This equation assumes simple radial equilibrium, a zero radial gradient of entropy in front and behind the vane, and an inlet axial-velocity distribution which is constant radially. The end-wall boundary layer was neglected in this calculation. For incompressible flow, the exit axial velocity of the mean radius was found by altering its value until the plot of exit axial velocity against the radius squared satisfied the continuity equation.

The turning angles which were used in selecting vane cambers and setting angles for guide vanes I and II from two-dimensional cascade data (ref. 4) were those calculated from exit axial and tangential velocities. In reference 5, it was found that, to get good correlation between two-dimensional cascade data and those flows in which there is a change in axial velocity across a blade row at each radial station, the three-dimensional flow velocity diagram at each radius should be modified to a diagram based on some constant axial velocity. A typical guide-vane velocity diagram is presented in figure 3. The best correlation occurred when the turning angle used to select the two-dimensional cascade sections and setting angles at a given radius was that obtained using the average of the inlet and exit velocities and the exit tangential velocity at that radius. This turning angle is shown in figure 3 as θ_M, the mean turning angle. Since guide vanes I and II were designed by use of turning angles based on exit axial velocities for selecting vane cambers and setting angles from cascade data, the design turning angles had to be redetermined. The turning angles which were originally used for applying cascade data were assumed to be those based on mean axial velocities. As a result, the design turning angles were determined by an iterative procedure using the previously mentioned guide-vane equation and continuity equation. This modification did not alter the design turning angles and velocities for vane I because the axial velocity is constant for incompressible flow across a vane with a vortex type of tangential velocity distribution. However, the design tangential velocities for vane II had a greater increase in tangential velocity with radius than the solid-body and, hence, the design axial velocity distributions indicated a greater amount of radial flow.

Blade III was designed with a solid-body type of tangential velocity distribution and the vane sections and setting angles were selected by use of turning angles based on the average axial velocity. All blade sections and setting angles were determined from low-speed cascade data (ref. 4). A summary of the blade design data is presented in table I and a comparison of the design tangential velocity distributions is presented in figure 4.

[redacted]

The actual tip solidity for designs II and III was 1.5. The tip blade sections used were not tested at quite this high a solidity in the investigation reported in reference 4. The cascade test data used for the tip blade sections were at the highest solidity for which test data were available (1.40 for the tip section of design II and 1.435 for the tip section of design III).

Calculations

Turning angles and absolute velocities at each of the circumferential positions at each radial station were obtained from the measured static and total pressures and flow angles. The absolute velocity was separated into its axial and tangential components. The axial components were arithmetically averaged around the circumference to obtain an average axial velocity at each radial station. The average tangential component at each radial station was obtained from a circumferential average of mass-weighted tangential velocities. The measured turning angle at each radial station was obtained by mass weighting those measured at all the circumferential positions at that radial station.

Design values of turning angle and axial velocity were obtained as described in the discussion of the blade design. Corrected design values of turning angle were obtained by the method of reference 1.

RESULTS AND DISCUSSION

Comparison between measured and design turning angles.- Measured and design turning-angle distributions are presented in figure 5 for designs I, II, and III. The design turning angles presented are those based on the exit axial velocity at each radius. The induced velocities caused by end-wall boundary layers and radial circulation gradients are neglected. A comparison of the design and measured turning-angle curves for the free-vortex guide vane (fig. 5(a)) shows good agreement in trend exclusive of the wall-boundary-layer region; however, the measured angles ranged from 0° to 3.0° above design values. In figures 5(b) and 5(c), measured turning angles are also above design, if the wall boundary layers and the tip region which are affected by three-dimensional secondary flow phenomena are ignored. This difference results from the selection of guide-vane blade sections and angles of attack from the two-dimensional cascade data of reference 4. Recent unpublished cascade tests of one of the sections reported in reference 4, the NACA 65-(12)10 blade section, indicated that the turning angles at a solidity of 1.5 were about 2° to 3° higher than those of reference 4. The higher turning angles obtained in the recent tests are probably a result of using blades of aspect ratio 2.0, as

compared with 1.0 for reference 4; hence, these recent tests represent more closely two-dimensional flow conditions. Turning-angle differences of this order of magnitude very likely exist for the other blade sections presented in reference 4. Therefore, if more nearly two-dimensional data had been used for selecting blade sections, very good agreement between measured and design turning angles would have resulted for vanes with circulation distributions similar to those of vanes I, II, and III, exclusive of the hub and tip regions affected by boundary layer and secondary flows.

In figure 5, all the measured turning-angle curves have variations in the regions adjacent to the inner and outer casings (inner 10 percent and outer 30 percent of guide vane). These variations are the result of secondary flow effects which are caused primarily by the circulation gradient along the vane and the end-wall boundary layer. The geometric location of these regions and the amount of variation between measured and predicted turning angles therein depends on the type and amount of radial circulation gradient and the development of the end-wall boundary layers.

For a free-vortex guide vane, the circulation decreases gradually from the midpoint of the guide vane to the wall boundary layer, and within the boundary layer, the circulation decreases rapidly close to the wall. The trailing-vortex system induces velocities which alter the turning angles expected from two-dimensional blade-section considerations. Since the circulation change for the free-vortex condition in the region exclusive of the boundary layer is not large and is approximately symmetrical about the blade midspan point, the trailing vortices which result from a combination of the blade vorticity and the end-wall boundary-layer vortices are not strong enough to affect appreciably the turning angles expected from two-dimensional considerations. Hence, only slight dips in the turning-angle curve are noticeable at the end walls of figure 5(a).

For those guide vanes having tangential velocities which increase with radius (designs II and III), excluding the wall boundary-layer regions, the maximum circulation occurs at the tip. Since circulation decreases rapidly close to the walls, the largest change in circulation occurs in the tip boundary layer; therefore, the shed vorticity and the resulting secondary induced effects are strongest in this region. As a result, figures 5(b) and 5(c) indicate much larger dips in measured turning angle and much larger regions affected by secondary flow phenomena near the tip than near the hub. The turning-angle dip that occurs in design II is similar to that of the solid-body design III because of their similar tangential velocity distributions. (See fig. 4.) A more complete discussion of secondary flows may be found in reference 1.

The effect of these secondary flow phenomena in designs II and III was to reduce the turning angles below the design values over the outboard

[redacted]

30-percent of the guide vanes. Hence, if the secondary flow phenomena are ignored in determining the guide-vane design for vanes having radial circulation gradients as great or greater than those of vanes II and III (fig. 6), actual turning angles as much as 7° below design may occur in the tip region. If the first-stage rotor is heavily loaded and operating very close to its critical Mach number at the tip, guide-vane turning angles which are lower than design would result in higher tip Mach numbers and angle of attack and, hence, could effect an appreciable reduction in compressor efficiency.

Comparison between measured and design velocity distributions.- The tangential and axial velocity distributions calculated from the measured data are presented with their respective design values in figure 7. Over the main-stream portion of the vanes, the tangential velocity components are consistently higher than design for all three vanes. This difference may be largely attributed to basing the designs on the low turning angles of reference 4, as previously discussed. A comparison of figure 7 with figure 5 indicates that the dip in the turning-angle distribution occurs as a dip in the tangential velocity distribution and a rise in the axial velocity distribution as is to be expected. It is evident from figure 7(a) that the sealing between the blades of vane I and the inner casing was not adequate and, consequently, the measured tangential velocities dropped below design in the hub region.

A comparison of the design and measured axial velocity distributions shows good agreement in trend; also, excluding the regions strongly affected by secondary flows, there is good numerical agreement. The differences are attributable to the accuracy of velocity measurements at the low speeds of these tests, the use of low turning angles of reference 4 for design purposes, and the assumption of simple equilibrium. Hence, the design method utilizing simple radial equilibrium in conjunction with two-dimensional cascade data gives good agreement between design and measured velocities and turning angle over the major portion of the vane (that portion not strongly affected by secondary flow effects), even for exit axial velocities at the hub two or three times greater than those at the tip.

Comparison between measured and corrected design turning angles.- The design turning angles were corrected for induced effects caused by end-wall boundary layers and the radial circulation gradient by the method of reference 1. Figure 8 presents measured and corrected values of turning angle plotted against radius. Figure 8(a) indicates that the correction method gives good agreement for the turning-angle trend for the free-vortex guide vane. The variation between measured and corrected design turning angles is about the same as that between measured and design turning angles of figure 5(a) and is attributed to the low values of turning angle presented in reference 4. Hence, the correction method of reference 1 works very well for the free-vortex type of guide vanes.

[redacted]

2M

In reference 1, good numerical agreement between measured and corrected turning angles was obtained for nonconstant circulation guide vanes for which maximum amount of radial variation of design axial velocity from hub to tip was relatively small (no greater than 17 percent). Guide vanes II and III of this paper had much larger radial variations in design axial velocity, that is, exit to inlet axial velocity ratios of $\left(V_{a_2}/V_{a_1}\right)_{hub} = 1.33$ and $\left(V_{a_2}/V_{a_1}\right)_{tip} = 0.42$ for design II and $\left(V_{a_2}/V_{a_1}\right)_{hub} = 1.31$ and $\left(V_{a_2}/V_{a_1}\right)_{tip} = 0.63$ for design III.

From a comparison of figures 5(b) and 8(b) and figures 5(c) and 8(c), the general numerical agreement between the measured and corrected turning-angle curves is not so good as between the measured and design curves. However, the trends predicted by the corrected turning-angle curves are much better than those of the design curves, particularly in the tip region where the secondary flow effects were more pronounced. It is likely that the numerical agreement between the corrected and measured turning-angle curves would be much improved if more accurate two-dimensional turning angles were available for the vane sections and setting angles used. The numerical difference between the corrected and measured turning angles for vanes II and III is only slightly greater than that which appears for vane I and in all cases is within the order of the discrepancy found in the turning angles of reference 4. Therefore, the method of reference 1 can be expected to give fairly good agreement even for guide vanes having large axial-velocity variations (hub axial velocities two or three times greater than those at the tip).

The guide-vane test data presented herein and in reference 1 cover a wide range of circulation distributions; hence, for guide vanes having circulation distributions within the range of those presented, the amount and extent of the turning-angle distortion can be obtained from a comparison of measured and design turning-angle distributions presented. If such guide vanes are to be incorporated into a compressor in which the performance could be seriously affected by not obtaining design guide vane turning angles in the tip region, the first-rotor design could be altered to take into account the distortion in the guide-vane velocity diagram. Any attempt to eliminate the tip-region turning-angle distortion by designing the tip region of the guide vane with some overturning could very likely be unsatisfactory since such adjustments increase the magnitudes and gradients of the design circulation which result in further increases in secondary flows and losses. Hence, the net gain from such adjustments is questionable.

Contour plots of total pressure loss.- Contour plots of total pressure loss behind the vane as a percent of inlet dynamic pressure are plotted for vanes I, II, and III in figure 9. Unfortunately, because of the construction of the cascade, it was difficult to obtain a smooth junction and tight seal between the hub casing and the vane. In

[redacted]

figure 9(a), the large very high-loss region near the hub casing may be attributed to inadequate sealing between the guide vane and the inner casing. Although this region appears to have little effect on turning angle near the hub of vane I, see figure 5(a), an appreciable effect on tangential and axial components of the absolute velocity may be noted in figure 7(a). Outside the hub region of vane I (fig. 9(a)), a small high-loss region occurs near the tip and the remaining wake loss covers a very narrow region. In figures 9(b) and 9(c), small high-loss regions may be noted near the hub casing (the seal between the vane and the casing being adequate) and a larger region of high loss near the tip casing, where the vane loading was greatest. As in the condition of vane I, the remaining wake loss of vanes II and III covers a narrow region. From a comparison of figures 9(a), 9(b), and 9(c), the amount of total pressure loss associated with designs II and III which had a great deal of radial flow (hub exit axial velocities approximately three times greater than that at the tip) is somewhat greater than that for the free-vortex guide vane (if the leakage loss region of vane I is disregarded). The effect of this increased loss on succeeding blade rows is not known since the loading that can be allowed in guide vanes before the succeeding blade rows are seriously affected has not been clearly defined.

Entering-wall boundary layers were less than 0.20 inch thick at hub and tip of all vanes. From figure 9, it may be seen that the wall-boundary-layer build-up through the blade passage was appreciable for designs II and III in which large amounts of radial flow were experienced; and for vanes having less radial flow than these designs, the wall-boundary-layer build-up would be proportionately less. At present the amount of boundary-layer build-up that can be allowed in guide-vane passages without seriously affecting the efficiency of the following rotor has not been determined.

SUMMARY OF RESULTS

The results of an investigation of secondary flows on the turning angles of three highly loaded inlet guide vanes having a free vortex, a solid body, and a design tangential velocity distribution which increased radially at a greater rate than the solid-body type are summarized as follows:

Measured turning angles as much as 7° below design values can result over the outboard 30-percent of the vane if the induced effects of secondary flows are ignored in designing highly loaded inlet guide vanes with large radial circulation gradients (hub axial velocity two or three times greater than that at the tip section).

The Lieblein and Ackley method for correcting two-dimensional turning-angle data for the effects of secondary flows gave good agreement between measured and corrected design turning angles for guide vanes having large variations in axial velocity (hub axial velocity two or three times greater than that at the tip).

The measured guide vane turning angles, in the regions where secondary flow effects were negligible, were always greater than the two-dimensional cascade turning angles reported by Zimney and Lappi (in some instances by as much as 3°); but the general agreement was good.

The total pressure loss associated with the guide vanes having a large amount of radial flow (hub axial velocity two or three times greater than that at the tip) is somewhat greater than that for a free-vortex guide vane. The effect of this increased loss on the performance of succeeding blade rows is not known.

The design method utilizing simple radial equilibrium and modifying the three-dimensional velocity diagram for vane-camber selection purposes gives good agreement over the major portion of the vane span (that portion not strongly affected by secondary flow effects), even for exit velocities at the hub two or three times greater than those at the tip section.

Langley Aeronautical Laboratory
National Advisory Committee for Aeronautics
Langley Field, Va.

[redacted]

REFERENCES

1. Lieblein, Seymour, and Ackley, Richard H.: Secondary Flows in Annular Cascades and Effects on Flow in Inlet Guide Vanes. NACA RM E51G27, 1951.

2. Carter, A. D. S.: Three Dimensional Flow Theories for Axial Compressors and Turbines. National Gas Turbine Establishment Rep. No. R.37, Ministry of Supply, Sept. 1948.

3. Savage, Melvyn, and Beatty, Loren A.: A Technique Applicable to the Aerodynamic Design of Inducer-Type Multistage Axial-Flow Compressors. NACA TN 2598, 1952.

4. Zimney, Charles M., and Lappi, Viola M.: Data for Design of Entrance Vanes From Two-Dimensional Tests of Airfoils in Cascade. NACA ACR L5G18, 1945.

5. Kahane, A.: Investigation of Axial-Flow Fan and Compressor Rotors Designed for Three-Dimensional Flow. NACA TN 1652, 1948.

[redacted]

TABLE I

DESIGN DATA FOR GUIDE VANES TESTED

Number of vanes, 24

	Design I			Design II			Design III		
	Hub	Pitch	Tip	Hub	Pitch	Tip	Hub	Pitch	Tip
Angle of attack, α, deg	32.4	22.4	16.1	13.0	21.0	36.3	15.5	22.0	35.4
Mean turning angle, θ_M, deg	45.9	34.6	27.3	19.7	33.1	56.0	22.2	34.1	49.1
Solidity, σ	1.44	1.47	1.50	1.50	1.50	1.50	1.50	1.50	1.50
Blade section	NACA 64-(B)06	NACA 64-(A)06	NACA 65-(12)06	NACA 65-(8)06	NACA 64-(A)06	NACA 64-(C)06	NACA 65-(8)06	NACA 64-(A)06	NACA 64-(B)06
Chord, in.	1.88	2.88	3.93	1.96	2.94	3.93	1.96	2.94	3.93

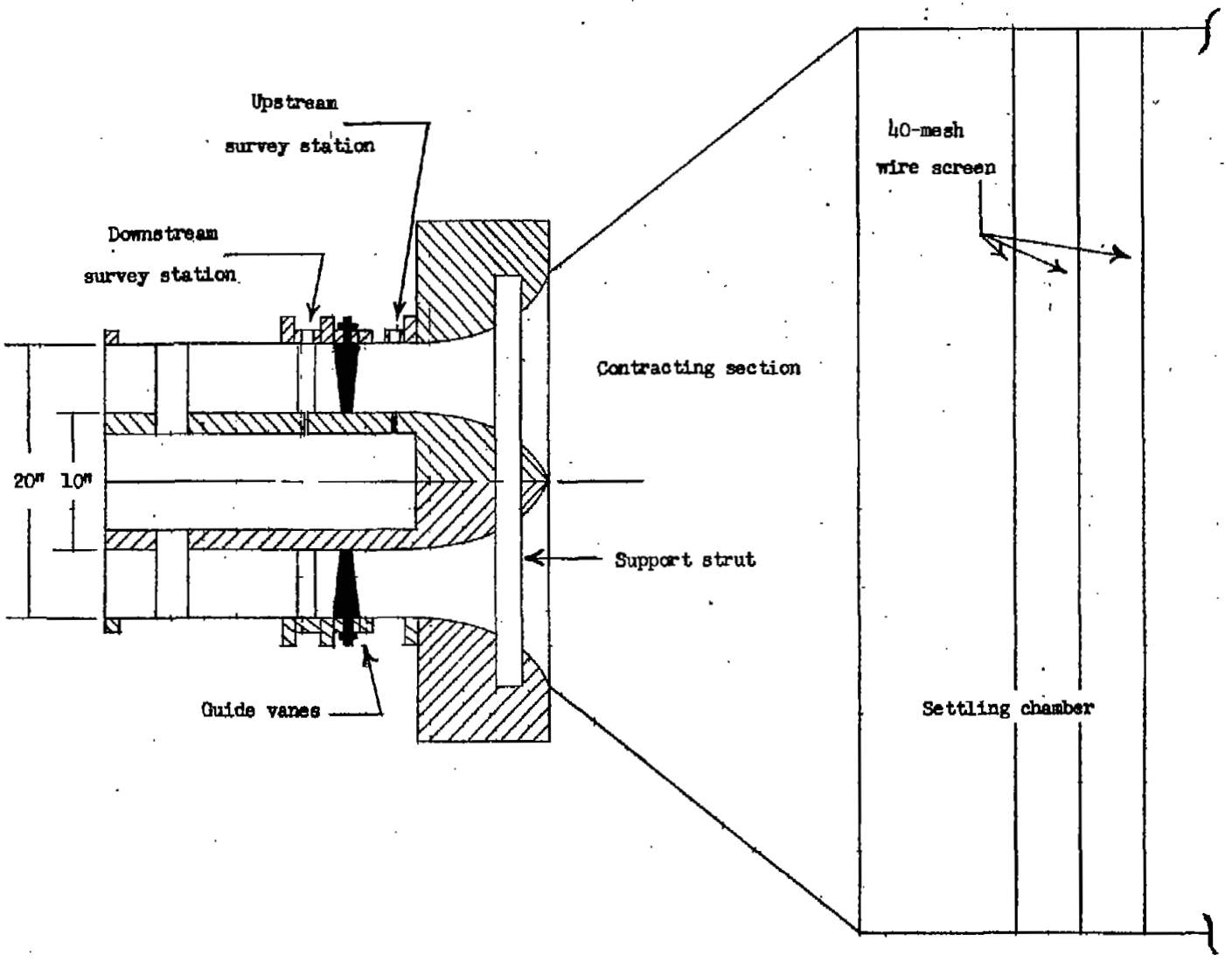

Figure 1.- Cross-sectional view of 20-inch annular cascade.

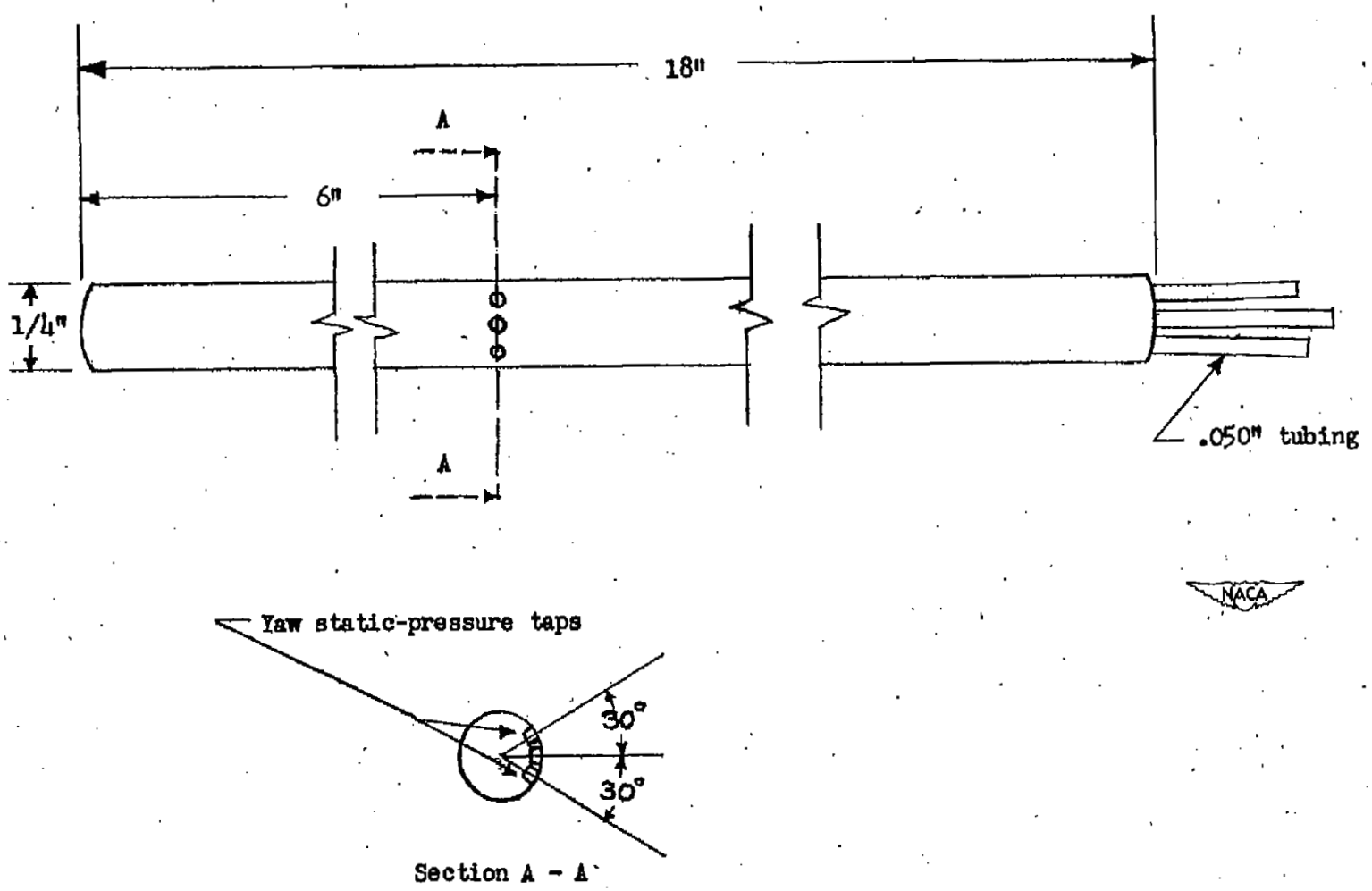

Figure 2.- Survey instrument.

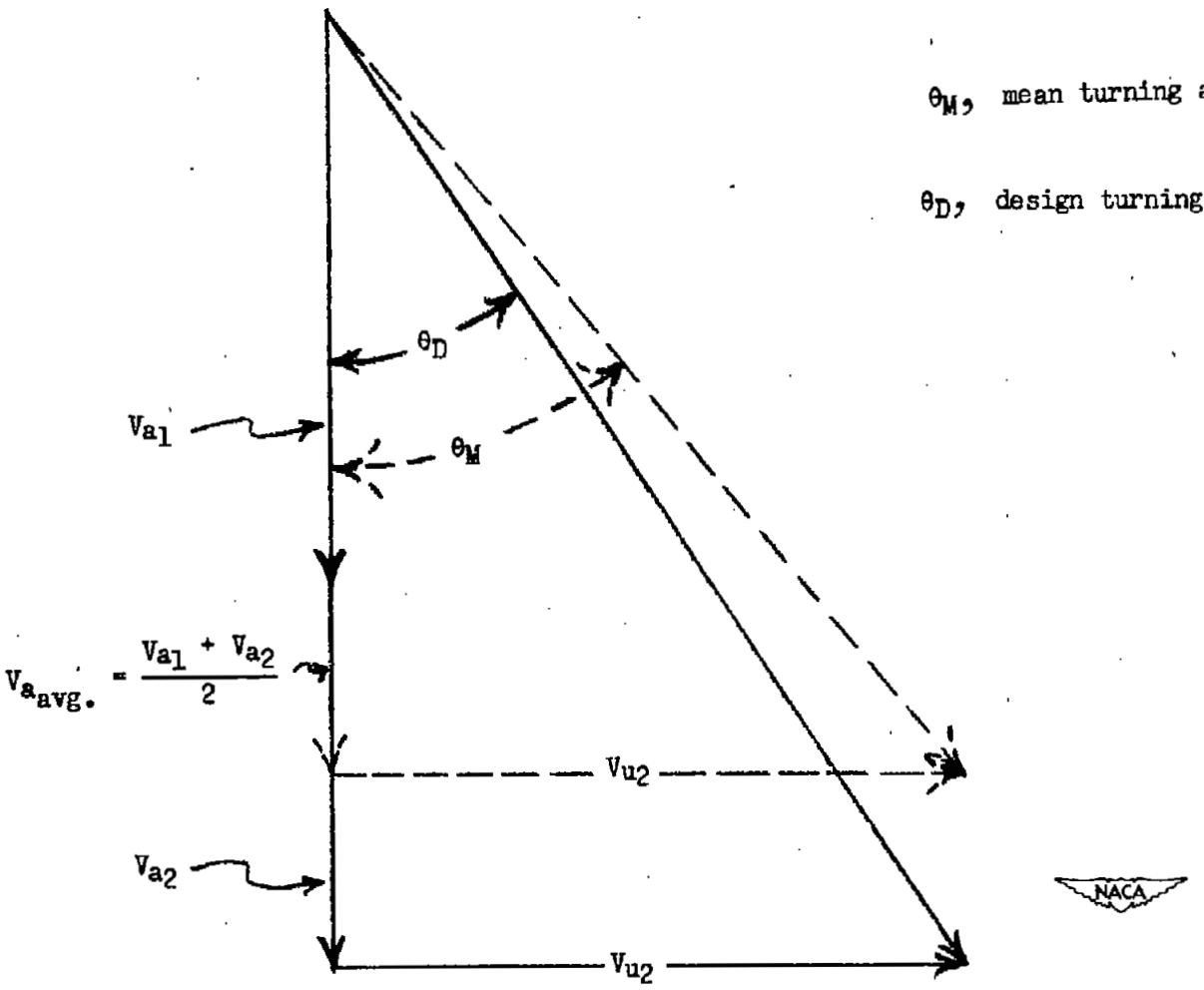

Figure 3.- Typical guide-vane velocity diagram at one radial station.

3M

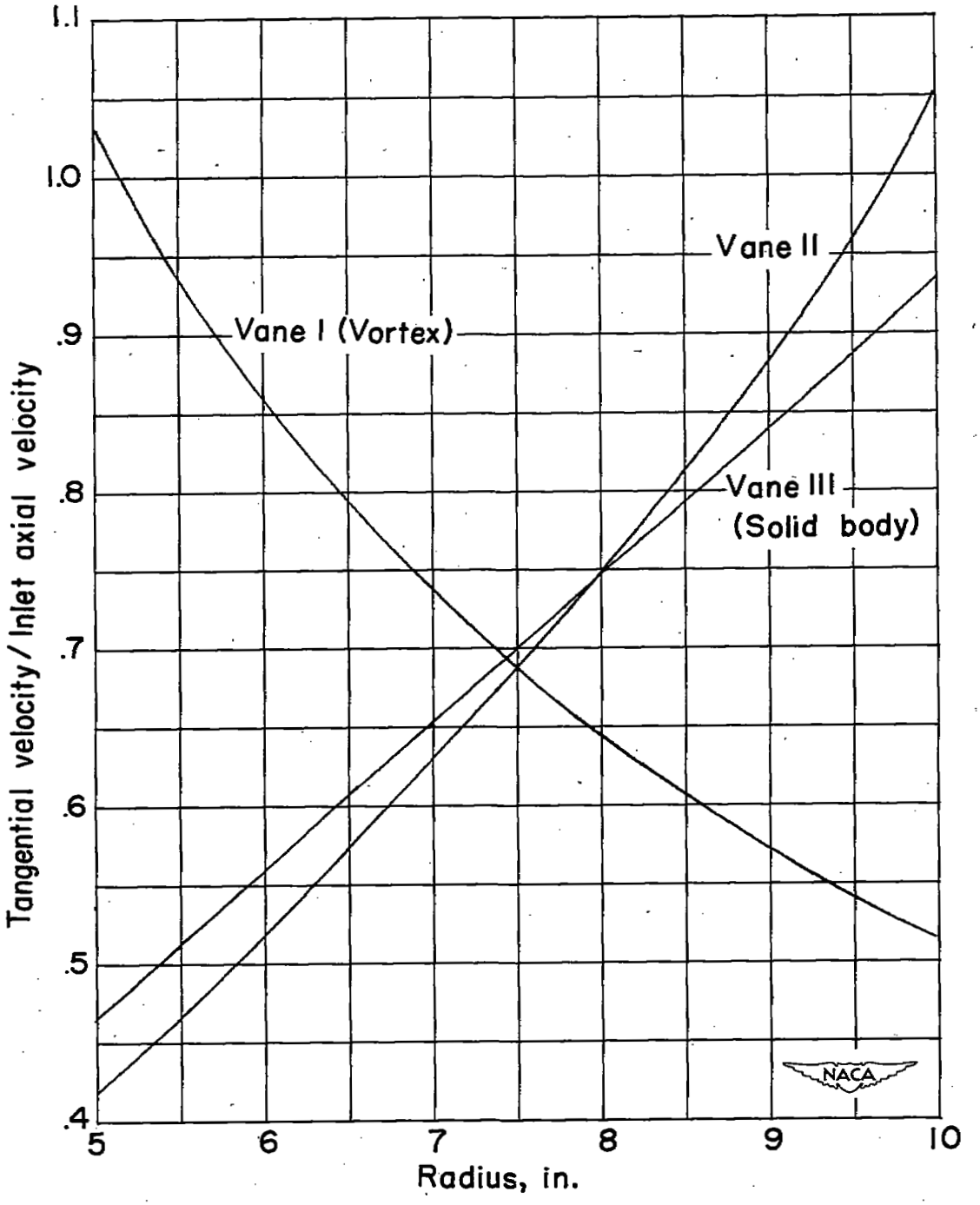

Figure 4.- Comparison of design tangential velocity distributions.

[redacted]

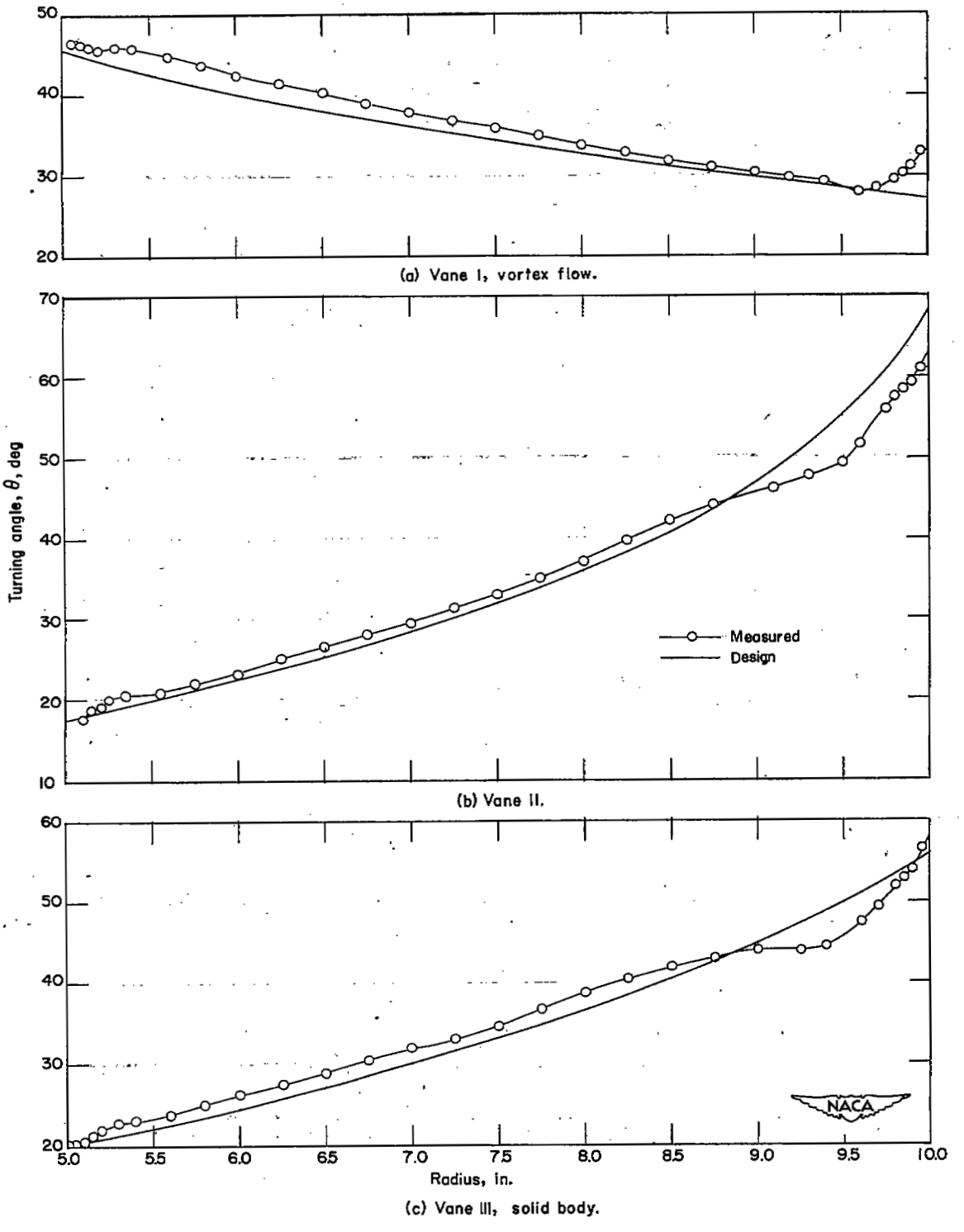

Figure 5.- Measured and design turning-angle distributions against radius.

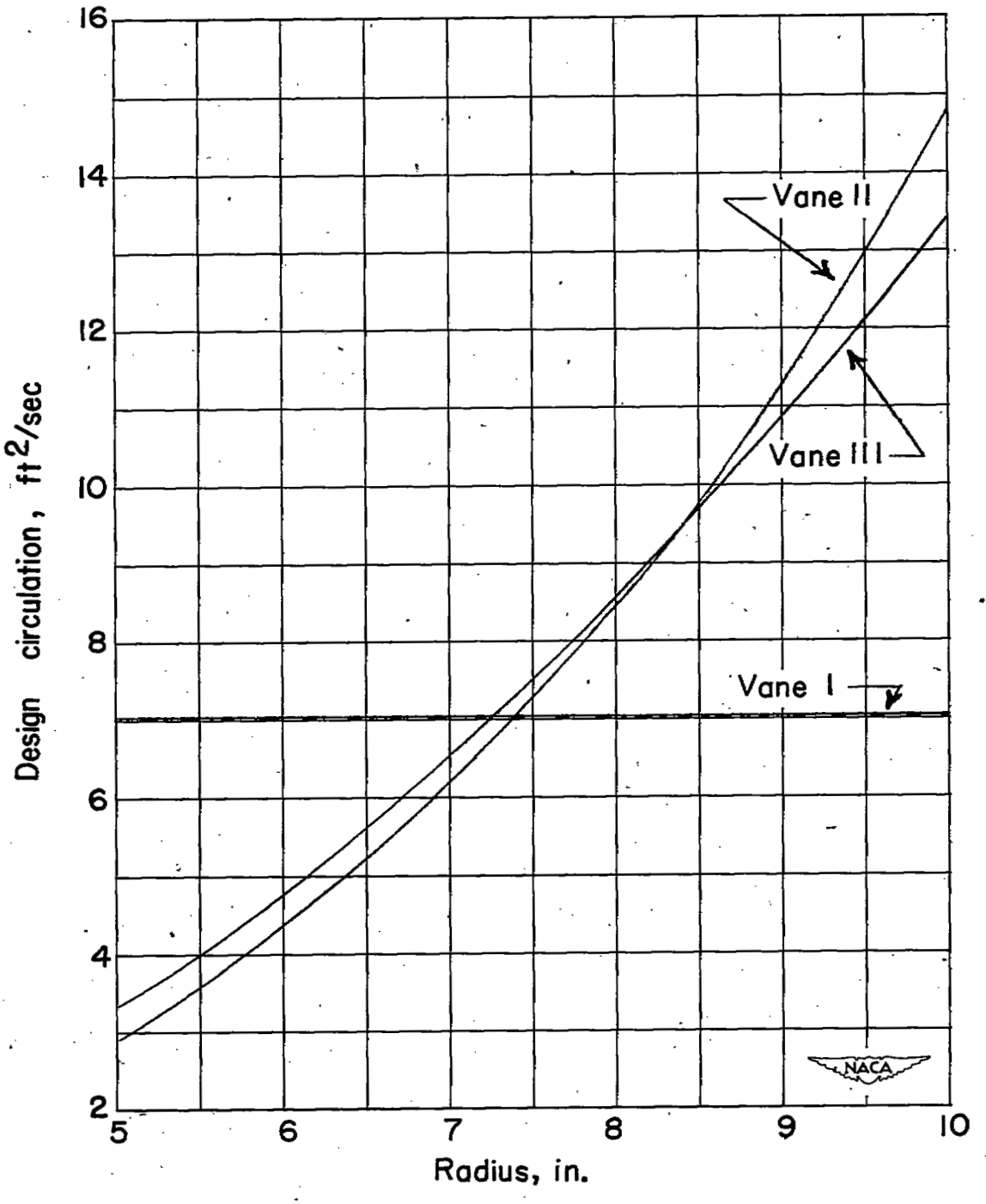

Figure 6.- Design circulation against radius for the three guide vanes tested.

[redacted]

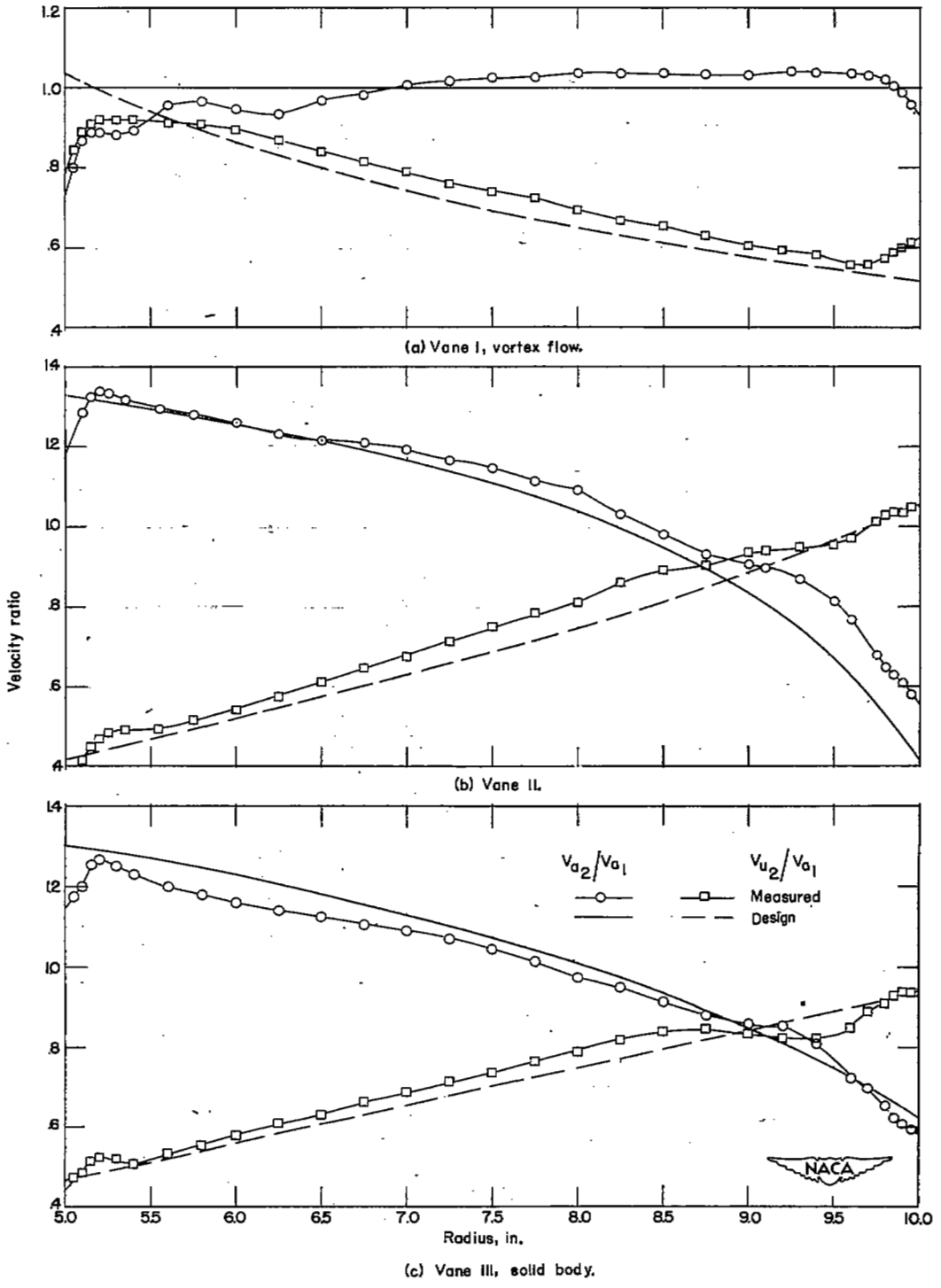

Figure 7.- Axial and tangential velocity distributions plotted against radius.

[redacted]

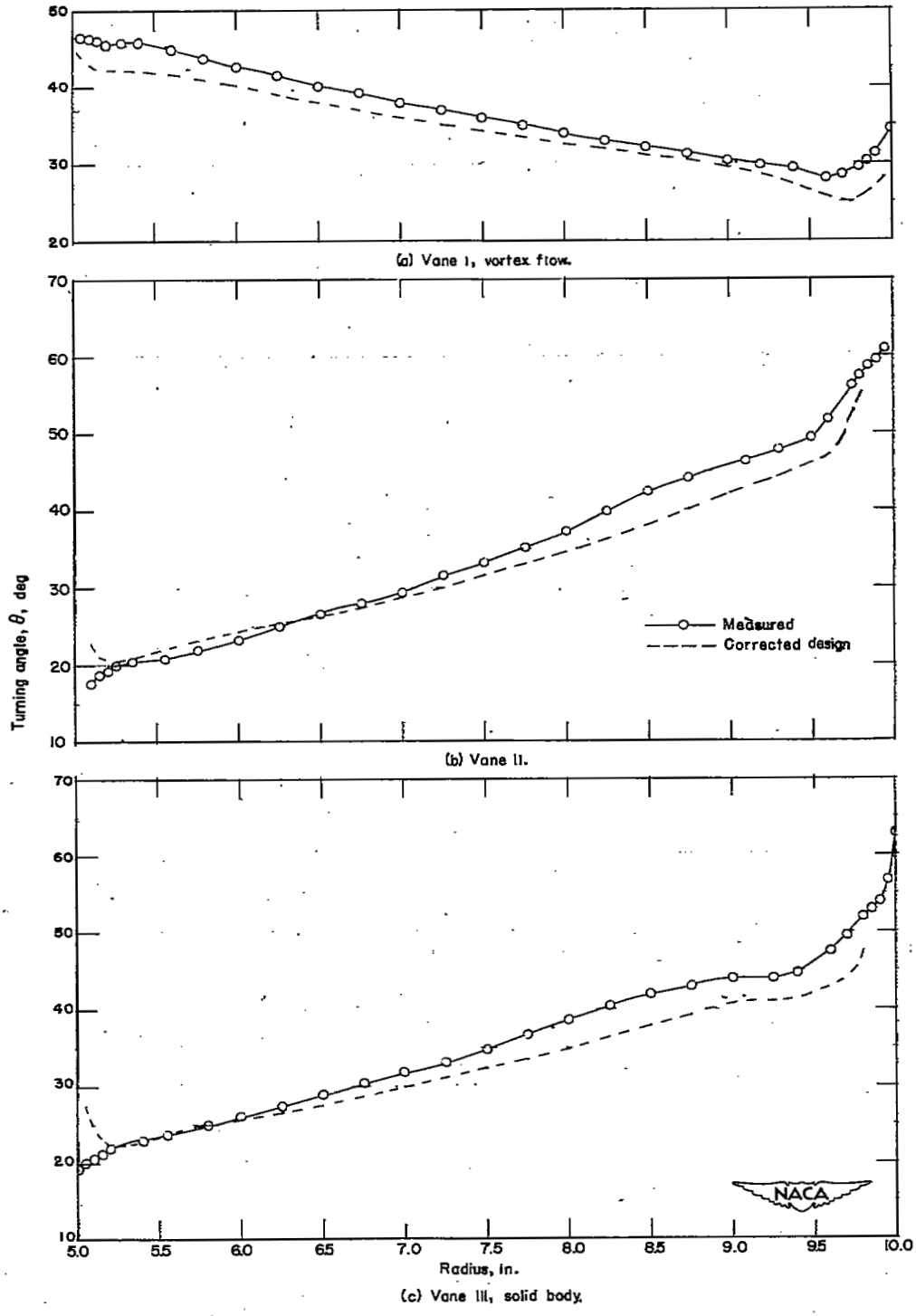

Figure 8.- Design turning-angle distributions corrected by the method of reference 1 and measured turning angle plotted against radius.

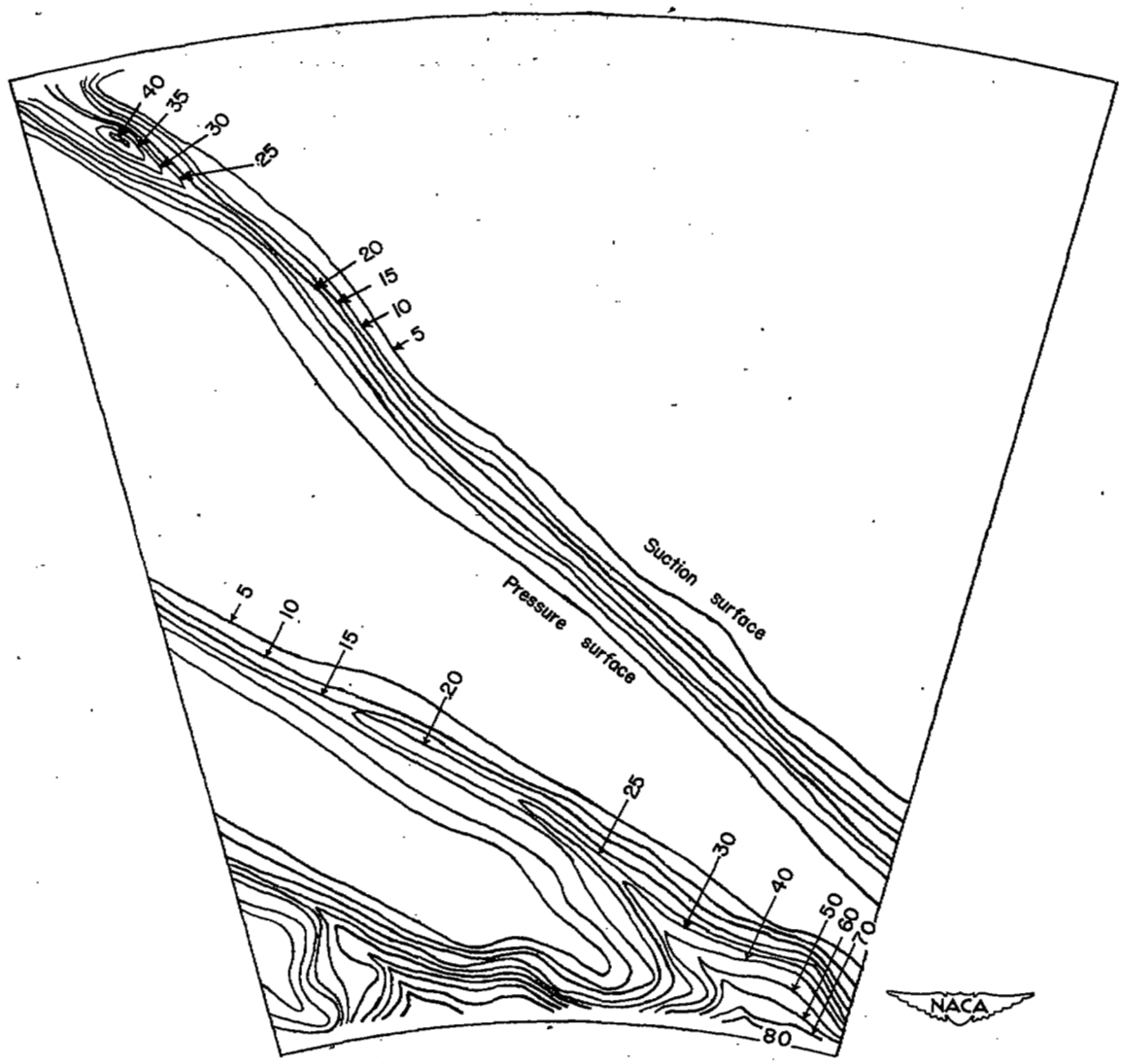

(a) Vane 1.

Figure 9.- Contour plot of total pressure loss behind the vane as a percent of inlet dynamic pressure.

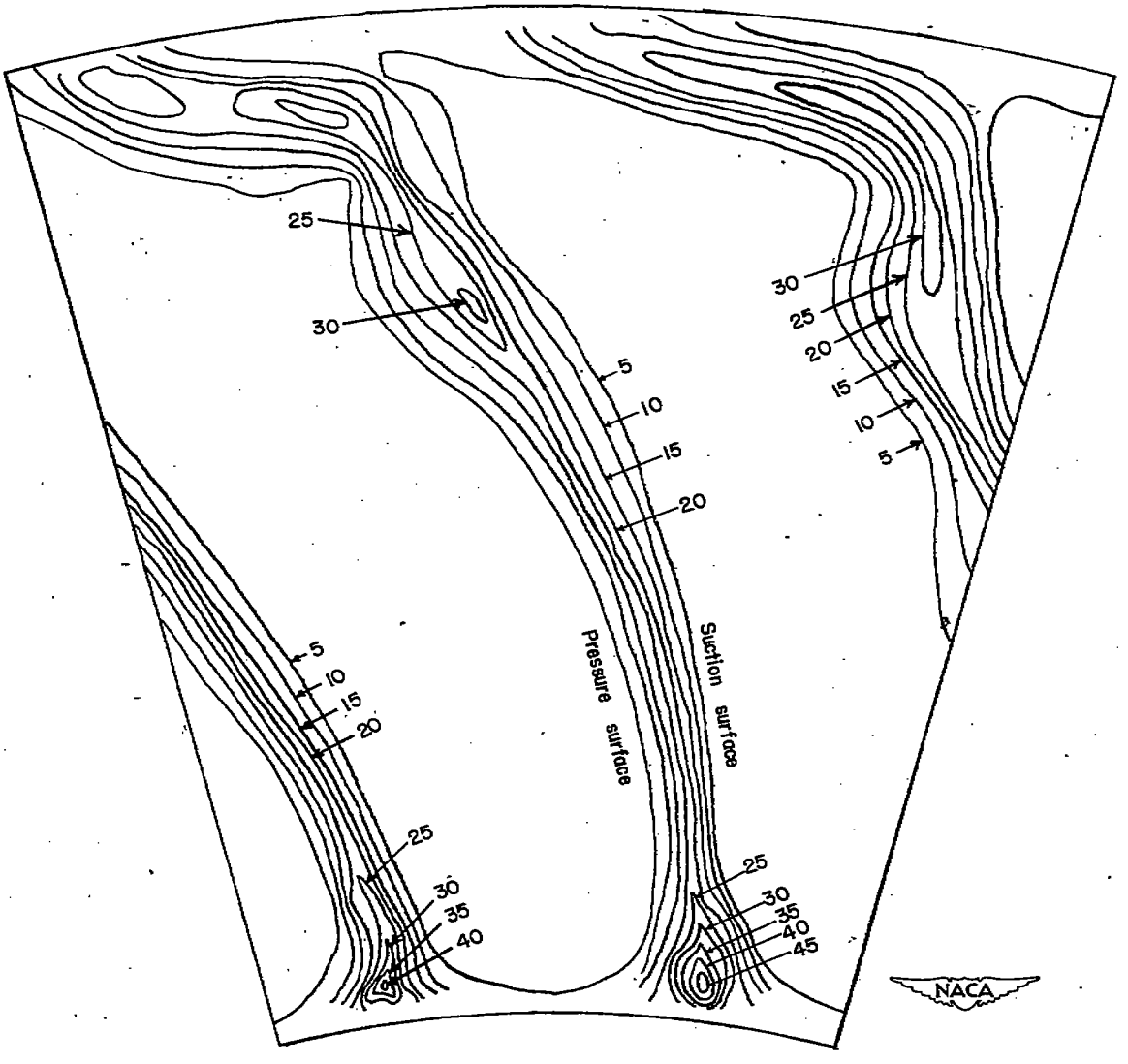

(b) Vane II.

Figure 9.- Continued.

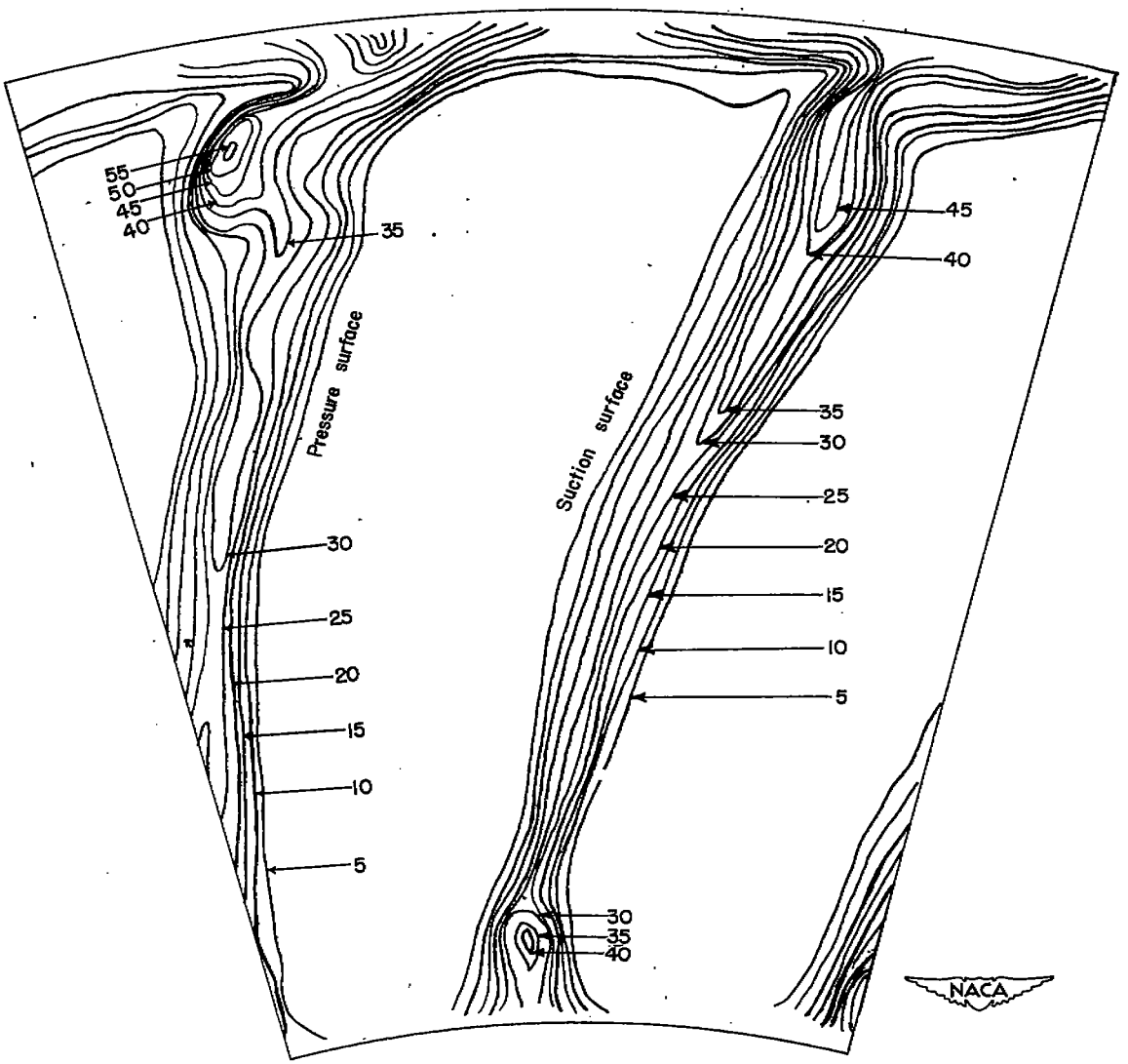

(c) Vane III.

Figure 9.- Concluded.

NACA-Langley - 7-28-52 - 350

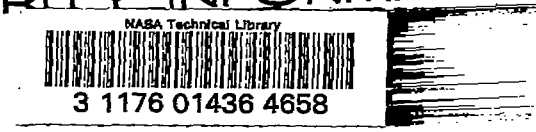

[redacted]